The inclusion complex of rosmarinic acid into beta-cyclodextrin: A thermodynamic and structural analysis by NMR and capillary electrophoresis

Amra Aksamija, Ange Polidori, Raphael Plasson, Olivier O. Dangles, Valérie Tomao

Food Chemistry (2016), Vol. 208, p. 258-263, DOI: 10.1016/j.foodchem.2016.04.008
Journal homepage : www.elsevier.com/locate/foodchem

The inclusion complex of rosmarinic acid into beta-cyclodextrin: A thermodynamic and structural analysis by NMR and capillary electrophoresis

Amra Aksamija [a], Ange Polidori [b], Raphaël Plasson [a], Olivier Dangles [a], Valérie Tomao [a,*]

[a] *University of Avignon, INRA, UMR408 SQPOV, 84000 Avignon, France*
[b] *University of Avignon, UMR5247 CBSA, 84000 Avignon, France*

A B S T R A C T

This work focuses on the characterization of the rosmarinic acid (RA)-β-cyclodextrin (CD) complex in aqueous solution by ^{1}H NMR (1D- and 2D-ROESY), completed with studies by capillary electrophoresis (CE). From the ^{1}H NMR data, the stoichiometry of the complex was determined by a Job's plot and the binding constant was estimated from a linear regression (Scott's method). At pH 2.9, the results showed that RA binds CD with a 1:1 stoichiometry and a binding constant K_b of 445 (±53) M^{-1} or 465 (±81) M^{-1} depending on the CD protons (H-5 or H-3) selected for the evaluation. The K_b value was also calculated from the CD-induced chemical shifts of each RA proton in order to collect information on the structure of the complex.

The pH dependence of K_b revealed that the RA carboxylic form displays the highest affinity for CD. An investigation by capillary electrophoresis fully confirmed these results. 2D ROESY analysis provided detailed structural information on the complex and showed a strong correlation between H-3 and H-5 of CD and most RA protons. In conclusion, RA, an efficient phenolic antioxidant from rosemary with a marketing authorization, spontaneously forms a relatively stable inclusion complex with CD in water.

Keywords:
Beta-cyclodextrin
Rosmarinic acid
Inclusion complex
NMR
ROESY
Capillary electrophoresis

1. Introduction

Naturally occurring phenolic compounds are currently used in the food industry as additives, especially in functional foods due to their potential health promotion in terms of antioxidant and anti-inflammatory protection (Campos-Vega, Guadalupe Loarca-Piña, & Oomah, 2010).

Rosmarinic acid (RA), an ester of caffeic acid and 3,4-dihydroxyphenyllactic acid, is a natural phenolic compound commonly found in many Lamiaceae herbs such as *Rosmarinus officinalis*, an aromatic evergreen shrub. Besides its antioxidant and anti-inflammatory activities, RA has antiallergenic, antiviral, and antibacterial properties and displays a very low toxicity (Petersen & Simmonds, 2003) and (Furtado, de Almeida, Furtado, Cunha, & Tavares, 2008). To fulfill the consumer demand for natural food additives, rosemary extracts have been recently accepted by the EU food additive legislation as effective and natural alternatives to synthetic antioxidants.

However, the effectiveness of these natural antioxidants depends on the preservation or improvement of their stability, bioactivity and bioavailability (Fang & Bhandari, 2010). Nano-encapsulation within food-grade macromolecules represents a remarkable mean to maintain the structural integrity and potentially enhance the bioavailability of these bioactive compounds (Munin & Edwards-Lévy, 2011). Cyclodextrins, a group of naturally occurring macrocyclic oligosaccharides, are convenient encapsulating material widely used in the food industry as additives for the stabilization of flavors and for the elimination of undesired tastes (Astray, Gonzalez-Barreiro, Mejuto, Rial-Otero, & Simal-Gándara, 2009). In particular, β-cyclodextrin (CD) has been listed as a safe food additive since 1998 (Szente & Szejtli, 2004). Inclusion of natural phenols into CD enables their protection against enzymatic oxidation and non-enzymatic oxidation by dioxygen and thus can extend their stability over time (Cravotto, Binello, Baranelli, Carraro, & Trotta, 2006).

Numerous analytical methods, such as spectroscopic, electrochemical or separation techniques, have been used for the characterization of the inclusion complexes and the estimation of the thermodynamic parameters of binding (Mura, (2014)). Among

* Corresponding author.
E-mail address: valerie.tomao@univ-avignon.fr (V. Tomao).

Food Chemistry (2016), Vol. 208, p. 258-263, DOI: 10.1016/j.foodchem.2016.04.008
Journal homepage : www.elsevier.com/locate/foodchem

these methods, ^{1}H NMR is the most widely used (Pessine, Calderini, & Alexandrino G.L., 2012).

In aqueous solution, CDs are able to form inclusion complexes with a variety of phenolic compounds such as hydroxytyrosol (López-García, López, Maya, & Fernández-Bolaños, 2010), baicalin (Li, Zhang, Chao, & Shuang, 2009), isoquercitrin (Wang et al., 2009), quercetin (Koontz, Marcy, O'Keefe, & Duncan, 2009), and caffeic acid (Zhang, Li, Zhang, & Chao, 2009). This ability is due to their cone-shaped structure with a relatively lipophilic inner cavity and hydrophilic outer surface. The main driving force in complex formation is the release of high-enthalpy water molecules from the CD cavity and the development of strong van der Waals host (CD) – guest (ligand) interactions (Loftsson, Jarho, Másson, & Järvinen, 2005). Water molecules are displaced by the more hydrophobic guest molecules with a concomitant decrease of CD ring strain (Szejtli, 1998).

However, only few papers have been published on the inclusion of RA into CDs. Celik et al. have studied the CD-RA binding and the corresponding changes in antioxidant capacity of RA in solution using UV-visible and fluorescence spectroscopies (Çelik, Özyürek, Tufan, Güçlü, & Apak, 2011). Recently, Medronho et al. reported for the first time an NMR study of the β-CD-RA interactions, giving insight on the complex structure (Medronho, Valente, Costa, & Romano, 2014); however, much higher values (by one order of magnitude) of the association constant were estimated in this work.

These conflicting results prompted us to revisit CD-RA binding. As RA could be encapsulated in CD for application in foods of variable acidity, we also investigated the pH-dependence of the CD-RA binding to compare the affinity of the carboxylic and carboxylate forms of RA for the macrocycle. In this work, the CD-RA inclusion complex (Fig. 1) was investigated by 1D and 2D (ROESY) ^{1}H NMR in order to refine the structural characterization of the complex. Additionally, a complementary study by CE was performed. The values of the binding constant (K_b) obtained by independent analytical tools (fluorescence spectroscopy, NMR and CE) in different studies (Çelik, 2011; Medronho et al., 2014 and this work) will be discussed.

The experimental conditions for the formation of the inclusion complex are consistent with the EU food additive legislation.

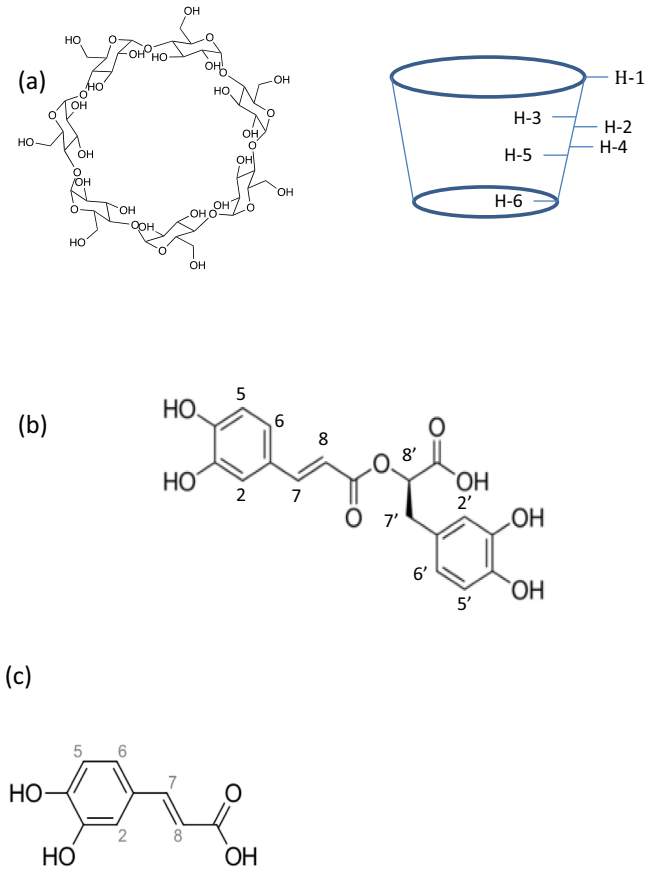

Fig. 1. Chemical structures of (a) β-cyclodextrin (CD), (b) rosmarinic acid (RA), (c) caffeic acid (CA).

2. Materials and methods

2.1. Materials

Rosmarinic acid, caffeic acid (CA), sodium dihydrogenphosphate dihydrate and disodium hydrogenphosphate heptahydrate were purchased from Sigma Aldrich (St. Louis, MO, USA). β-Cyclodextrin was kindly given by Roquette Freres (Lestrem, France). Sodium hydroxide was purchased from Prolabo (BDH Prolabo, VWR International, Haasrode, Belgium). Phenol was obtained from Carlo Erba (Carlo Erba Reagents, SdS, Peypin, France). D_2O for NMR analyses was purchased from Euriso-Top (Saint-Aubin, France). Demineralized water was obtained from VWR (VWR International S.A.S, France). Standard solutions for capillary conditioning, 0.1 M and 1.0 M NaOH solutions were supplied by Fluka Biochemika (Sigma-Aldrich Chemie, GmbH, Steinheim, Germany) while milliQ water was produced by an EASY pure RF compact ultrapure water system (Barnstead, ThermoFicher Scientific, Waltham, MA, USA). All reagents were of analytical grade quality.

2.2. NMR study

All RA and CD solutions were freshly prepared in D_2O. For the Job's plot, different volumes of 10 mM solutions of RA and CD in D_2O were mixed together to a constant volume keeping the sum of the total RA and CD concentrations equal to 10 mM.

For the determination of the apparent association constant (Scott's plot), two different series of samples were prepared.

In the first one, different volumes of a 1 mM CD solution in D_2O and of a solution containing RA (10 mM) and CD (1 mM) in D_2O were mixed together to a constant volume with a final RA/CD ratio ranging from 0.8 to 9.2.

In the second series, different volumes of a 1 mM RA solution and of a solution containing CD (10 mM) and RA (1 mM) in D_2O were mixed together to a constant volume with a final CD/RA ratio ranging from 0.8 to 9.2. Final solutions were equilibrated at room temperature and protected from light before measurement.

1D ^{1}H NMR spectra were recorded on a Bruker AC-400 MHz spectrometer (software Bruker Top Spin 2.1). 2D-ROESY spectra were recorded in on a Bruker AVL 600 MHz (Spectropole, Aix-Marseille University).

Chemical shifts are given in ppm (δ) and calculated using the internal reference of the HDO signal at 4.79 ppm. In all cases, the complexation-induced chemical shift difference is defined as the difference between the chemical shift of the free molecule to the chemical shift of bound molecule, $\Delta\delta = \delta_{free} - \delta_{complex}$.

2.3. Capillary Electrophoresis study

Electrophoresis experiments were performed using an automated capillary electrophoresis system (Beckman P/ACE MDQ, Fullerton, CA). Fused-silica capillaries (50 μm i.d. × 60 cm, 50 cm to the detector) were used.

Phosphate buffer (pH 7) for CE analysis was prepared with sodium dihydrogenphosphate dihydrate and disodium hydrogenphosphate heptahydrate in milliQ water (ionic strength = 10 mM) and stored at 4 °C. Working buffers were prepared by diluting up to 15 mM of CD in this phosphate buffer.

Stock solutions of RA and CA, both in final concentration equal to 5 mM, were prepared in milliQ water and protected from light at 4 °C. Sodium thiosulphate (1 mM) was added to protect the stock solutions against oxidation. Sonication of the stock solutions in an ultrasonic bath (5 min) was necessary to achieve complete solubility. The stock RA and CA solutions were renewed every 15 days. Samples for analysis were prepared by dilution of these stock solutions in milliQ water. After dilution, the concentrations were 0.05 mM for RA, 0.2 mM for CA and 1 mM for phenol.

Prior to first use, new capillaries were conditioned by flushing at 20 psi with milliQ water (2 min), 0.1 M NaOH (10 min), 1.0 M NaOH (5 min), milliQ water (2 min), then with working buffer for 15 min. In order to remove potentially adsorbed analytes, the capillary was rinsed with milliQ water (2 min), 0.1 M NaOH (5 min), milliQ water (2 min) and working buffer (5 min) every three consecutive runs. Before each sample run, the capillary was flushed with 0.1 M NaOH (1 min) and working buffer (5 min) and, after analysis, with working buffer (2 min). The capillary was thermostated at 20 °C. The sample was injected in hydrodynamic mode at 0.5 psi for 5 s and each analysis was performed under an applied voltage of 10 kV. Any measurement was repeated at least three times in identical conditions.

3. Results and discussion

3.1. Stoichiometry of the inclusion complex

The stoichiometry of inclusion complex between RA and CD was determined by using the method of continuous variations (Job's plot).

The CD protons that are most sensitive to bound RA are H-3 and H-5, as both points toward the interior of the cavity. The significant diamagnetic shift observed for those protons is essentially due to the magnetic anisotropy effects of RA's π-electrons in agreement with the formation of an inclusion complex (Ali & Upadhyay, 2008; Schneider, Hacket, & Rudiger, 1998). Table S1 shows the chemical shifts differences of H-5 (CD) for a CD mole fraction (r_{CD}) ranging from 0.1 to 0.9. It is also noteworthy that the aromatic protons H-2, H-6, H2′ and H-6′ of RA are also diamagnetically shifted. By contrast the other CD protons (H-1, H-2, H-4 and H-6), mostly localized outside the CD cavity, experience insignificant chemical shift variations. The superposition of the NMR spectra shows a significant shielding of the internal protons H-3 and H-5 of CD (Fig. 2). The stoichiometry of the inclusion complex was determined by plotting $r_{CD} \times \Delta\delta$ (H-3, CD) against r_{CD} by using the Job's method (Fig. S1). The symmetry of the curve obtained and its maximum at $r_{CD} = 0.5$ both point to a single complex of 1:1 stoichiometry. The same conclusion was reached with H-5. These results are in agreement with previous investigations by fluorescence spectroscopy (Çelik, 2011) and NMR (Medronho et al., 2014).

3.2. Stability of the inclusion complex

The apparent binding constant K_b was calculated according to the conventional Scott's equation assuming 1:1 binding.

$$\frac{[RA]}{\Delta\delta_{obs}} = \frac{[RA]}{\Delta\delta_{max}} + \frac{1}{K_b \Delta\delta_{max}} \quad (1)$$

$\Delta\delta_{obs}$ represents the observed chemical shift difference of CD proton H-3 or H-5 between free CD and the CD + RA mixtures.

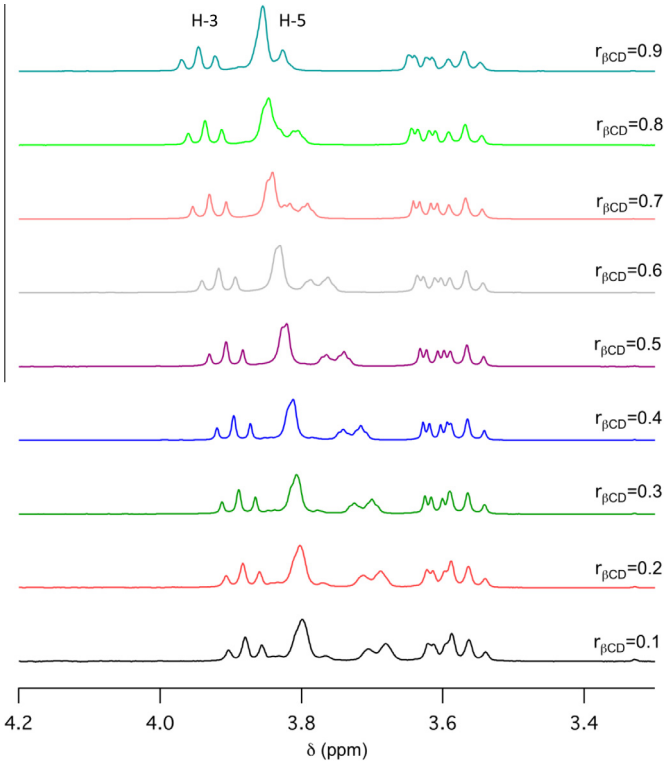

Fig. 2. Expansion of the ^{1}H NMR spectrum showing the displacement of H-5 and H-3 (CD) for a CD mole fraction (*r*CD) ranging from 0.1 to 0.9 in D_2O at pH 2.9. Different volumes of 10 mM solutions of RA and CD were mixed together to a constant volume keeping the sum of the total RA and CD concentrations equal to 10 mM in D_2O at pH 2.9.

$\Delta\delta_{max}$ is the chemical shift difference at saturation. The $[RA]/\Delta\delta_{obs}$ ratio for H-5 was plotted as a function of [RA], thus resulting in an excellent linear fit (Fig. 3). This confirms the 1:1 stoichiometry of the inclusion complex in agreement with the Job's plot. From the slope of the plot, one obtains: $\Delta\delta_{max} = 0.22 \pm 0.01$ ppm. The same plot with H-3 yields: $\Delta\delta_{max} = 0.10 \pm 0.01$ pm. The slope-to-intercept ratio equals the binding constant. From the H-5 and H-3 plots respectively, one obtains: $K_b = 445 \pm 53\ M^{-1}$ and $465 \pm 81\ M^{-1}$. As expected, both values are identical within experimental error.

RA displays two phenolic rings and each of them may be involved in the binding. A second series of measurements, in which RA is in low and constant concentration (1 mM) and CD in variable

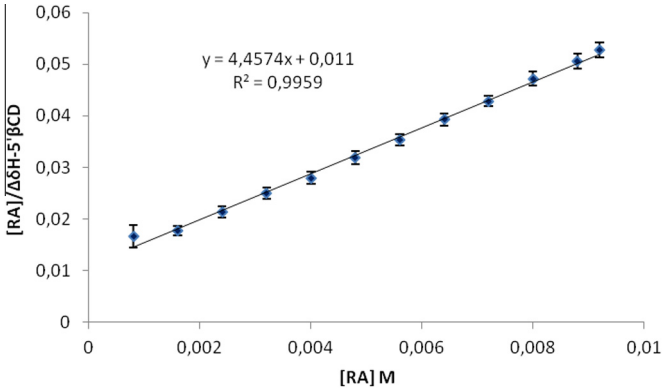

Fig. 3. Scott's plot for CD proton H-5 with CD concentration set at 1 mM and variable RA concentration in D_2O at pH 2.9.

concentration, was performed to collect information on the structure of the complex. Although the CD-induced chemical shift displacements of the RA protons are weak, Scott's plots could be constructed to estimate $\Delta\delta_c$ and K_b. The K_b values thus obtained are slight lower than the one obtained by monitoring the CD protons (Table S2). The latter are considered more reliable based on the higher sensitivity of the CD protons (especially H-5) to RA-CD binding, which is obvious from the larger $\Delta\delta_{max}$ values.

3.3. Structure of the inclusion complex

The assignments of RA protons were made on the basis of their specific coupling constants and on the COSY spectrum. The complete ^{1}H NMR data for each of RA protons is presented in the Table S3 and is consistent with those previously obtained in the literature (Lecomte, Giraldo López, Laguerre, Baréa, & Villeneuve, 2010). Analysis of the NMR spectrum of RA (1 mM) shows signals of six aromatic protons (H-2, H-5, H-6 and H-2′, H-5′, H-6′), two vinylic protons (H-7, H-8) and three aliphatic protons (H7′$_a$, H7′$_b$ and H-8′).

In Fig. S2, the ^{1}H NMR data show the large variations induced by RA on the chemical shifts of the CD protons located inside the cavity (H-3, H-5), compared with the weak variations of the CD protons located outside (H-1, H-2, H-4). Upon complex formation, the large shielding of H-3 and H-5 reflects the presence of one of the RA aromatic rings in the CD cavity.

In Fig. S3, the ^{1}H NMR data of free and bound RA are compared. Maximal CD-induced deshielding occurs for aromatic protons.

The geometry of the RA-CD complex was further investigated via a ROESY experiment. Two different mixing times were used to obtain the NOE correlations between RA (350 ms) and CD (150 ms) (Fig. 4). As expected from the 1D NMR spectra, strong correlations were observed between the CD H-3 and H-5 protons on the one hand and most of the RA protons on the other hand, especially H-2′ and H-5′ but also H-2. No correlation was observed between the RA protons and the protons of the CD outer surface (H-2, H-4). These results confirm without ambiguity the encapsulation of RA inside the CD cavity. The correlations between the CD protons and all RA aromatic protons suggest that both phenolic moieties can interact with the CD cavity. It can thus be assumed that two inclusion complexes are formed, one involving the caffeoyl moiety (complex 1, binding constant K_1) and the other one involving the 3.4-dihydroxyphenyllactic moiety (complex 2, binding constant K_2), both being in fast equilibrium via free RA. Overall, only a single averaged NMR spectrum is observed for the three species.

The observed chemical shift of any RA proton can be expressed as: $\delta_{obs} = x_0\delta_0 + x_1\delta_1 + x_2\delta_2$, δ_0, δ_1 and δ_2 being the chemical shifts of the proton in free RA, complex 1 and complex 2, respectively, and x_0, x_1 and x_2 the corresponding mole fractions.

Simple solution chemistry gives:

$$\delta_{obs} = \frac{\delta_0 + (\delta_1 K_1 + \delta_2 K_2)[CD]}{1 + (K_1 + K_2)[CD]} = \frac{\delta_0 + \delta_{max} K_b [CD]}{1 + K_b [CD]} \quad (2)$$

With $K_b = K_1 + K_2$ and $\delta_{max} = \frac{\delta_1 K_1 + \delta_2 K_2}{K_1 + K_2}$

Therefore, whatever the proton signal detected, the apparent binding constant derived from the chemical shift variations is the same and equals the sum of the individual binding constants. It can thus be assumed that differences in K_b values depending on the RA proton detected merely reflect differences in sensivity.

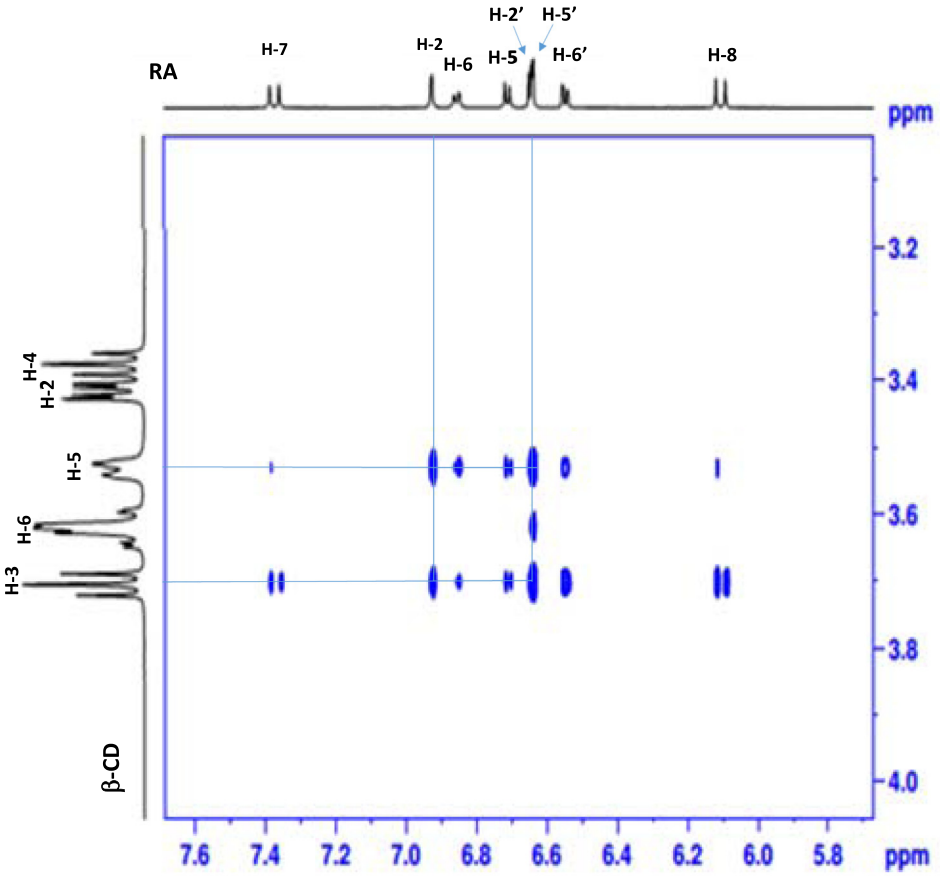

Fig. 4. ROESY spectrum of the 1:1 RA-CD complex (5 mM of each partner) in D_2O at pH 2.9 (mixing time = 150 ms).

However, it can be noted that the NOE correlations are especially intense between with the CD H-3 and H-5 protons and the vinylic protons of the caffeoyl part, which suggests a deep inclusion of this moiety into the cavity.

3.4. pH dependence of binding

The pH-dependence of the CD-RA complexation was investigated. At pH 2.9, RA is a mixture of neutral carboxylic (RA-CO_2H) and anionic carboxylate (RA-CO_2^-) forms in nearly equal proportions. When the pH was decreased to 1 (pure RA-CO_2H), the K_b values deduced from Scott's plots for the RA protons (variable CD concentration) were significantly higher. By contrast, when the pH was increased to 6 (pure RA-CO_2^-), the K_b values were lower.

Clearly, the less hydrophilic carboxyl form display a higher affinity for the CD cavity than the corresponding carboxylate. On the other hand, at pH 1 and 6, the Job's plots confirmed the 1:1 stoichiometry of the inclusion complex (data not shown). As shown in Table 1, the K_b values obtained at pH 6 (ca. 200 M^{-1}) are of the same order of magnitude as those obtained by Celik et al. (164 M^{-1}) by fluorescence but much lower than those obtained by Medronho et al. by NMR. Indeed, at pH 6, Medronho et al. have estimated K_b at ca. 1180 M^{-1} and 2030 M^{-1} depending on which RA aromatic ring is monitored and interpreted this difference by assuming two complexes in solution, the first one involving the caffeoyl moiety and the second the 3.4-dihydroxyphenyllactic moiety. As stated above, this interpretation is incorrect as both complexes are indistinguishable by NMR due to fast chemical exchange. Hence, differences in K_b values must be ascribed to differences in sensitivity depending on the protons monitored and techniques adopted (detection on RA at variable CD concentration *vs*. detection on CD at variable RA concentration).

3.5. Analysis of RA-CD inclusion complexes by capillary electrophoresis

To confirm the NMR data, the RA-CD inclusion complex was also studied by CE. The electrophoretic mobility of RA was measured in buffered CD solutions at different concentrations (Li and Waldron, 1999). The binding kinetics being fast with respect to the separation time, the measured mobility μ is the average mobility of the free (μ_{RA}) and bound (μ_{RA-CD}) RA forms:

$$\mu = (1-\alpha)\cdot\mu_{RA} + \alpha\cdot\mu_{RA-CD} \quad (3)$$

α being the bound fraction of RA. For a large CD-to-RA molar ratio, the free CD concentration can be considered constant and equal to the total CD concentration C, so that the binding constant can be expressed as:

$$K_b = \frac{[RA-CD]}{[RA][CD]} = \frac{\alpha}{(1-\alpha)\cdot C} \quad (4)$$

Hence, the measured electrophoretic mobility can be expressed as a function of C:

$$\mu = \frac{\mu_{RA} + K_b C\cdot\mu_{RA-CD}}{1+K_b C} \quad (5)$$

On top of binding effects, an increase in CD concentration leads to an increase in the buffer viscosity (Paduano, Sartorio, Vitagliano, & Costantino, 1990), and this in turn influences all the electrophoretic mobilities, which are inversely proportional to the buffer viscosity (Plasson & Cottet 2005). The electroosmotic flow μ_{eof} being inversely proportional to the buffer viscosity too (Corradini & Sprecacenere, 2003), it was used for evaluating the viscosity correction factor to be applied to the measured electrophoretic mobilities (Li and Waldron, 1999). A linear relationship between the elution time of a neutral marker (phenol) t_{eof} and the CD concentration was observed (correlation coefficient $R = 0.92$). It corresponds to a linear variation of the viscosity with a maximal variation of 8% for a CD concentration of 15 mM.

The K_b values can be obtained from the non-linear curve-fitting of the plot expressing the viscosity-corrected electrophoretic mobility μ as a function of C according to Eq. (5), thus enabling the determination of the numerical values of μ_{RA}, μ_{RA-CD} and K_b. The same method was repeated with caffeic acid (CA) for comparison purposes, as CA is structurally related to RA (see Fig. 1). The measurements were performed at 20 °C. The pH was fixed at 7 so as to ensure that the carboxyl groups of RA and CA are fully deprotonated. The ionic strength was fixed to a low value of 10 mM in order to avoid any heating of the capillary. Moreover, in those conditions, the ionic and actual electrophoretic mobilities can be taken equal (Plasson & Cottet, 2005).

The non-linear curve fitting yields: $K_b = 197$ (±14) M^{-1}, $\mu_{RA} = 1.520$ (±0.006) × 10^{-8} $m^2V^{-1}s^{-1}$ and $\mu_{RA-CD} = 0.934$ (±0.014) × 10^{-8} $m^2V^{-1}s^{-1}$ for RA, $K_b = 176$ (±4) M^{-1}, $\mu_{CA} = 2.101$ (±0.003) × 10^{-8} $m^2V^{-1}s^{-1}$ and $\mu_{CA-CD} = 1.047$ (±0.014) × 10^{-8} $m^2V^{-1}s^{-1}$ for CA (see Fig. 5).

The similar K_b values for RA and CA suggest that the caffeoyl moiety of RA is mostly responsible for the affinity of RA for CD and that the less polarizable dihydroxyphenyllactic moiety experiences a weaker binding. Taking hydroxytyrosol as a structural analog of the dihydroxyphenyllactic moiety, it can actually be noted that this olive phenol only weakly binds CD with a K_b value of ca. 90 M^{-1} (López-García et al., 2010).

Table 1
Maximal CD-induced ^{1}H NMR chemical shift displacements ($\Delta\delta_{max} = \delta_{max} - \delta_0$ (no CD)) of RA protons and binding constant (K_b) at variable pH values in D_2O (RA concentration = 1 mM).

	pH 1		pH 2.9		pH 6	
RA proton	$\Delta\delta_{max}$ (ppm)	K_b (M^{-1})	$\Delta\delta_{max}$ (ppm)	K_b (M^{-1})	$\Delta\delta_{max}$ (ppm)	K_b (M^{-1})
H-2	0.08	320	0.01	265	0.14	209
H-2′	0.08	352	0.06	316	0.012	319
H-5	0.09	314	0.02	260	0.4	256
H-5′	0.03	328	0.03	325	0.03	284
H-6	0.07	300	0.09	260	0.13	202
H-6′	0.09	330	0.06	328	0.02	238
H-7	0.03	342	0.02	313	0.03	222
H-7′	0.05	468	0.03	390	0.04	230
H-8	0.11	466	0.09	393	0.07	227
H-8′	0.11	466	0.08	299	0.07	227

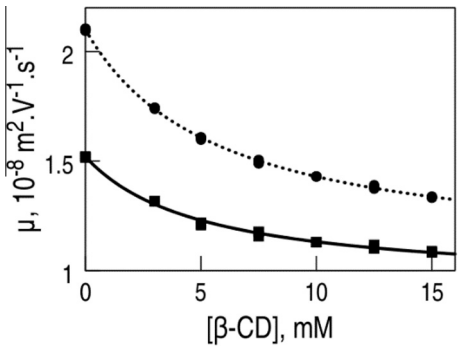

Fig. 5. Variation of the electrophoretic mobility of RA (solid line and squares) and CA (dotted line and circles) as a function of the total CD concentration, in phosphate buffer at pH 7, 20 °C, I = 10 mM, [RA] = 0.05 mM, [CA] = 0.2 mM. Circles and squares are experimental measurements for respectively CA-CD and RA-CD, each of them being repeated three times. The lines were obtained by non-linear curve-fitting of experimental data using Eq. (5).

The electrophoretic mobilities can also be used to evaluate the hydrodynamic radius of each species (Plasson & Cottet, 2005):

$$r_i = \frac{q}{6\pi\eta\mu_i} \quad (6)$$

with q the electric charge of the compounds (1.6×10^{-19} C) and η the water viscosity at 20 °C (10^{-3} Pa.s). This gives rRA = 5.6 Å, r_{CA} = 4.0 Å, rRA$_{-CD}$ = 9.1 Å, $r_{CA\text{-}CD}$ = 8.1 Å. These values can be compared with the hydrodynamic value of β-CD: r_{CD} = 7.7 Å (Pavlov, Korneeva, Smolina, & Schubert 2010). They are consistent with the inclusion of either RA or CA inside the β-CD cavity, as evidenced by a slight radius increase from free β-CD to the CA-β-CD and RA-β-CD complexes.

Close K_b values are thus obtained for RA-β-CD with this method and with the NMR method in neutral conditions (about 200 M^{-1}, see Table 1) with a similar precision (about 10% error).

This value is also in good agreement with the one determined by Celik et al. by fluorescence (164 ± 65 M^{-1}) rather than with the value obtained by NMR by Medrohno et al. (ca. 2000 M^{-1}). The consistency of EC methods with fluorescence methods was furthermore checked by performing a similar study for the association of RA with methyl-β-CD. A K_b value of 372 (±20) M^{-1} was determined; once again, this value is in perfect agreement with the value measured by Celik et al. (328 ± 39 M^{-1}).

4. Conclusion

The complementary use of 1D and 2D ROESY NMR and EC methods have led to consistent results concerning the complex formation between RA and β-CD. In all conditions, a mixture of 1:1 complexes in fast equilibrium was obtained, both catechol subunits of RA being potentially inserted inside the CD hydrophobic cavity, while no interactions of RA with the outside of the CD unit could be reliably detected. Typically, the apparent binding constant is ca. 450 M^{-1} at pH 2.9 (equimolar mixture of the carboxyl and carboxylate forms), corresponding to an encapsulation efficiency of ca. 50% when the two species are mixed in an equimolar concentration of 5 mM each. The pH dependence of K_b shows that the carboxyl form of RA displays a higher affinity for the macrocycle than the carboxylate form.

In conclusion, RA forms a relatively stable complex with β-CD, especially in acidic conditions. By accommodating the catechol nuclei inside the CD cavity, the binding could inhibit their interactions with redox-active metal traces, thereby providing higher stability for food applications. The binding could also modulate the release of RA in the digestive tract as a function of pH.

Acknowledgements

The authors thank Roquette Freres (Lestrem, France) for providing β-cyclodextrin.

Appendix A. Supplementary data

Supplementary data associated with this article can be found, in the online version, at http://dx.doi.org/10.1016/j.foodchem.2016.04.008.

References

Ali, S. M., & Upadhyay, S. K. (2008). Complexation studies of pioglitazone hydrochloride and β-cyclodextrin: NMR (^{1}H, ROESY) spectroscopic study in solution. *Journal of Inclusion Phenomena and Macrocyclic Chemistry, 62*, 161–165.
Astray, G., Gonzalez-Barreiro, C., Mejuto, J. C., Rial-Otero, R., & Simal-Gándara, J. (2009). A review on the use of cyclodextrins in foods. *Food Hydrocolloids, 23*, 1631–1640.
Çelik, S. E., Özyürek, M., Tufan, A. N., Güçlü, K., & Apak, R. (2011). Spectroscopic study and antioxidant properties of the inclusion complexes of rosmarinic acid with natural and derivative cyclodextrins. *Spectrochimca Acta A Molecular Biomolecular Spectroscopy, 78*, 1615–1624.
Corradini, D., & Sprecacenere, L. (2003). Dependence of the electroosmotic flow in bare fused-silica capillaries from pH, ionic strength and composition of electrolyte solutions tailored for protein capillary zone electrophoresis. *Chromatographia, 58*, 587–596.
Cravotto, G., Binello, A., Baranelli, E., Carraro, P., & Trotta, F. (2006). Cyclodextrins as food additives and in food processing. *Current Nutrition and Food Science, 2*, 343–350.
Fang, Z., & Bhandari, B. (2010). Encapsulation of polyphenols. *Trends in Food Science & Technology, 21*, 510–523.
Furtado, M. A., de Almeida, L. C. F., Furtado, R. A., Cunha, W. R., & Tavares, D. C. (2008). Antimutagenicity of rosmarinic acid in Swiss mice evaluated by the micronucleus assay. *Mutation Research, 657*, 150–154.
Koontz, J. L., Marcy, J. E., O'Keefe, S. F., & Duncan, S. E. (2009). Cyclodextrin inclusion complex formation and solid-state characterization of the natural antioxidants α-tocopherol and quercetin. *Journal of Agriculture and Food Chemistry, 57*, 1162–1171.
Lecomte, J., Giraldo López, L. J., Laguerre, M., Baréa, B., & Villeneuve, P. (2010). Synthesis, characterisation and free radical scavening properties of rosmarinic acid fatty esters. *Journal of the American Oil Chemists Society, 87*, 615–620.
Li, J., & Waldron, K. C. (1999). Estimation of the pH-independent binding constants of alanylphenylalanine and leucylphenylalanine stereoisomers with β-cyclodextrin in the presence of urea. *Electrophoresis, 20*, 171–179.
Li, J., Zhang, M., Chao, J., & Shuang, S. (2009). Preparation and characterization of the inclusion complex of Baicalin (BG) with β-CD and HP-β-CD in solution: An antioxidant ability study. *Spectrochimica Acta Part A, 73*, 789–793.
Loftsson, T., Jarho, P., Másson, M., & Järvinen, T. (2005). Cyclodextrins in drug delivery. *Expert Opinion on Drug Delivery, 2*, 335–351.
López-García, M. Á., López, Ó., Maya, I., & Fernández-Bolaños, J. G. (2010). Complexation of hydroxytyrosol with β-cyclodextrins. An efficient photoprotection. *Tetrahedron, 66*, 8006–8011.
Medronho, B., Valente, A. J. M., Costa, P., & Romano, A. (2014). Inclusion complexes of rosmarinic acid and cyclodextrins stoichiometry, association constants, and antioxidant potential. *Colloid and Polymer Science, 292*, 885–894.
Munin, A., & Edwards-Lévy, F. (2011). Encapsulation of natural polyphenolic compounds. *Pharmaceutics, 3*, 793–829.
Mura, P. (2014). Analytical techniques for characterization of cyclodextrin complexes in aqueous solution. *Journal of Pharmaceutical and Biomedical Analysis, 101*, 238–250.
Paduano, L., Sartorio, R., Vitagliano, V., & Costantino, L. (1990). Diffusion properties of cyclodextrins in aqueous solution at 25 °C. *Journal of Solution Chemistry, 19*, 31–39.
Pavlov, G. M., Korneeva, E. V., Smolina, N. A., & Schubert, U. S. (2010). Hydrodynamic properties of cyclodextrin molecules in dilute solutions. *European Biophysics Journal, 39*, 371–379.
Pessine, F. B., Calderini, A., & Alexandrino, G. L. (2012). a review: Cyclodextrin inclusion complexes probed by NMR techniques. In D. H. Kim (Ed.), *Magnetic resonance spectroscopy*. InTech Publishing.
Petersen, M., & Simmonds, M. S. (2003). Rosmarinic acid. *Phytochemistry, 62*, 121–125.
Plasson, R., & Cottet, H. (2005). Determination of homopolypeptide conformational changes by the modeling of electrophoretic mobilities. *Analytical Chemistry, 77*, 6047–6054.
Campos-Vega, Rocio., Guadalupe Loarca-Piña, B., & Oomah, Dave. (2010). Minor components of pulses and their potential impact on human health. *Food Research International, 43*, 461–482.
Schneider, H., Hacket, F., & Rudiger, V. (1998). NMR studies of cyclodextrins and cyclodextrin complexes. *Chemical Reviews, 98*, 1755–1785.
Szejtli, J. (1998). Introduction and general overview of cyclodextrin chemistry. *Chemical Reviews, 98*, 1743–1753.
Szente, L., & Szejtli, J. (2004). Cyclodextrins as food ingredients. *Trends in Food Science & Technology, 15*, 137–142.
Wang, Y., Qiao, X., Li, W., Zhou, Y., Jiao, Y., Yang, C., Dong, C., et al. (2009). Study on the complexation of isoquercitrin with β-cyclodextrin and its derivatives by spectroscopy. *Analytica Chimica Acta, 650*, 118–123.
Zhang, M., Li, J., Zhang, L., & Chao, J. (2009). Preparation and spectral investigation of inclusion complex of caffeic acid with hydroxypropyl-β-cyclodextrin. *Spectrochimica Acta Part A, 71*, 1891–1895.